

Supporting Information

S 1 SEM investigations of X% Mo:BiVO₄ thin films deposited on Si substrates. X represents the amount in atomic percent of Mo in the synthesis solution.

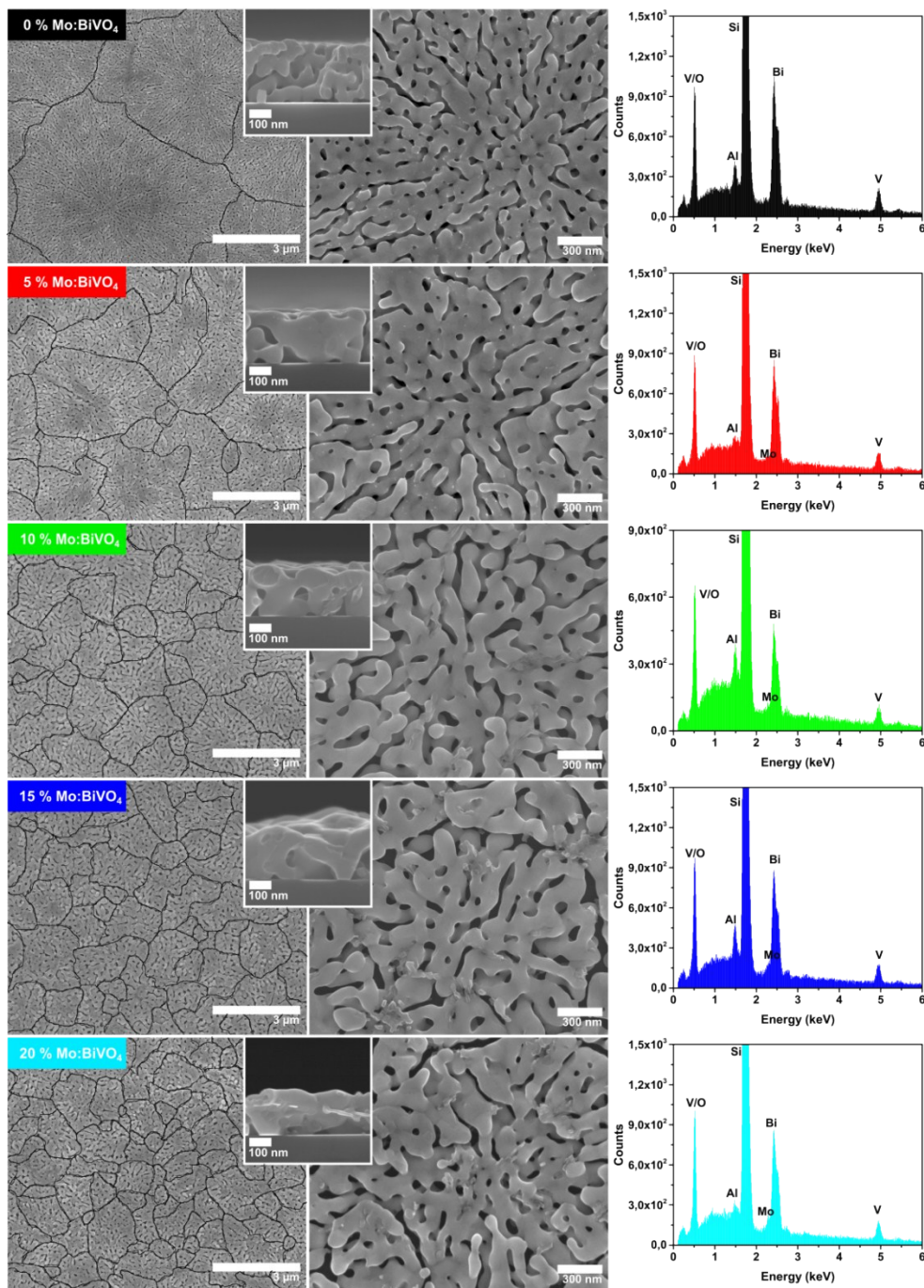


Figure S 1. SEM investigations of X% Mo:BiVO₄ thin films deposited on Si substrates. X (0%, 5%, 10%, 15%, 20%) represents the amount in atomic percent of Mo in the synthesis solution. Grooves separating domains from each other were highlighted.

S 2 UV/Vis spectra of synthesis solutions containing different amounts of Mo precursor

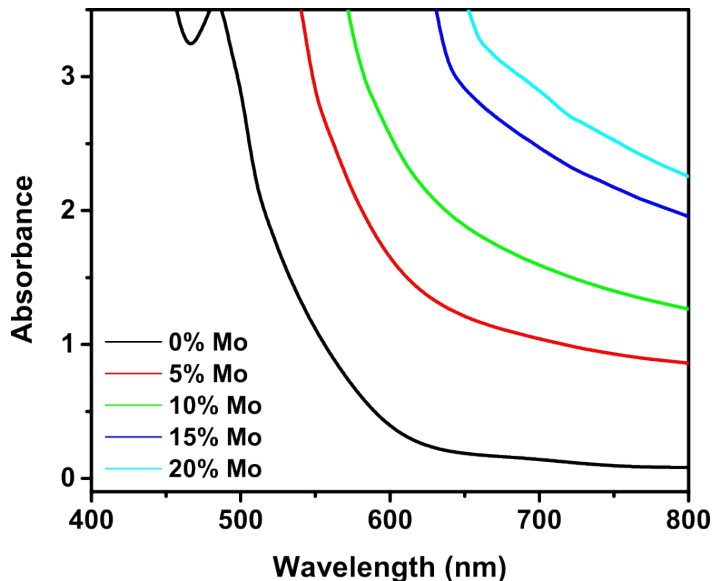


Figure S 2. UV/Vis spectra of synthesis solutions containing different amounts (at % regarding Bi) of Mo precursor. High level of absorbance is a consequence of dramatically increased light scattering and absorption by non-dissolved Mo precursor within the solution.

S 3 Known phase transitions and reference XRD patterns for BiVO₄

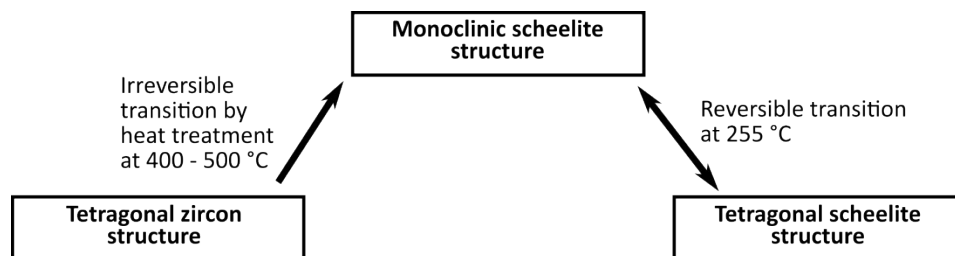


Figure S 3. Known phase transitions for BiVO₄ acc. to S. Tokunaga, H. Kato, A. Kudo, *Chem. Mater.* 2001, 13, 4624–4628.

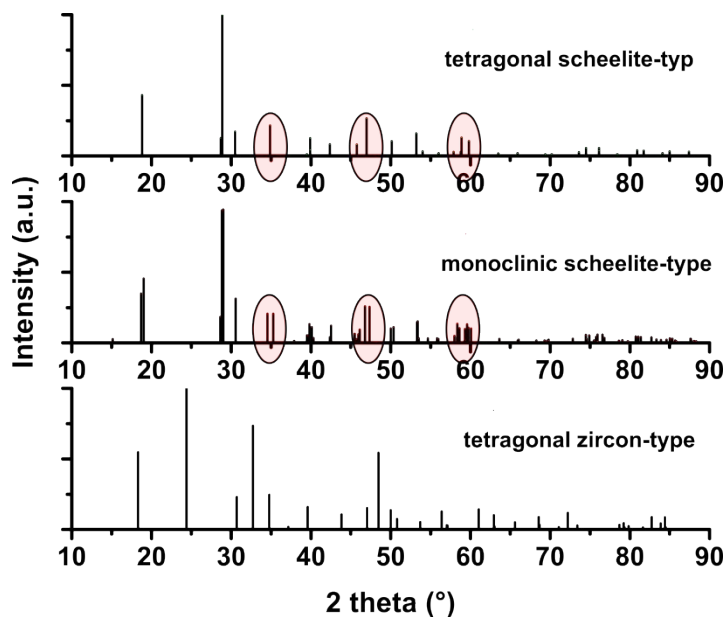


Figure S 4. Reference XRD pattern for the known crystal structures for BiVO_4 : tetragonal zircon type (PDF 00-014-0133), monoclinic scheelite type (PDF 00-014-0688) and tetragonal scheelite type (PDF 00-048-0774). Selected reflections allowing to distinguish between monoclinic scheelite-type and tetragonal scheelite-type are highlighted.

S 4 Structural analysis

Table S 1. Refined structural parameters of BiVO_4 powders in comparison to 5 %, 10 %, 15% and 20% Mo: BiVO_4 powders.

Composition	0% Mo: BiVO_4	5% Mo: BiVO_4	10% Mo: BiVO_4	15% Mo: BiVO_4	20% Mo: BiVO_4
Crystal system	monoclinic				tetragonal
Space group	$I2/b$				$I4_1/a$
Formular units	$Z=4$				$Z=4$
Lattice parameters	$a = 5.1930(6)\text{Å}$ $b = 5.1019(6)\text{Å}$ $c = 11.7028(3)\text{Å}$ $\gamma = 90.333(2)^\circ$	$a = 5.1839(5)\text{Å}$ $b = 5.1188(5)\text{Å}$ $c = 11.6959(10)\text{Å}$ $\gamma = 90.238(2)^\circ$	$a = 5.1741(4)\text{Å}$ $b = 5.1412(4)\text{Å}$ $c = 11.6917(9)\text{Å}$ $\gamma = 90.144(3)^\circ$	$a = 5.1673(4)\text{Å}$ $b = 5.1532(4)\text{Å}$ $c = 11.6855(8)\text{Å}$ $\gamma = 90.094(4)^\circ$	$a=b = 5.1634(2)\text{Å}$ $c = 11.6825(3)\text{Å}$ $\gamma = 90^\circ$
Unit cell volume	$V = 310.05(7)\text{Å}^3$	$V = 310.35(5)\text{Å}^3$	$V = 311.01(4)\text{Å}^3$	$V = 311.16(4)\text{Å}^3$	$V = 311.46(2)\text{Å}^3$
R_{wp}	0.0296	0.0263	0.0256	0.0240	0.0285
R_{Bragg}	0.0286	0.0302	0.0267	0.0278	0.0307
R_{exp}	0.0107	0.0105	0.0103	0.0103	0.0098
S	2.79	2.49	2.48	2.32	2.91

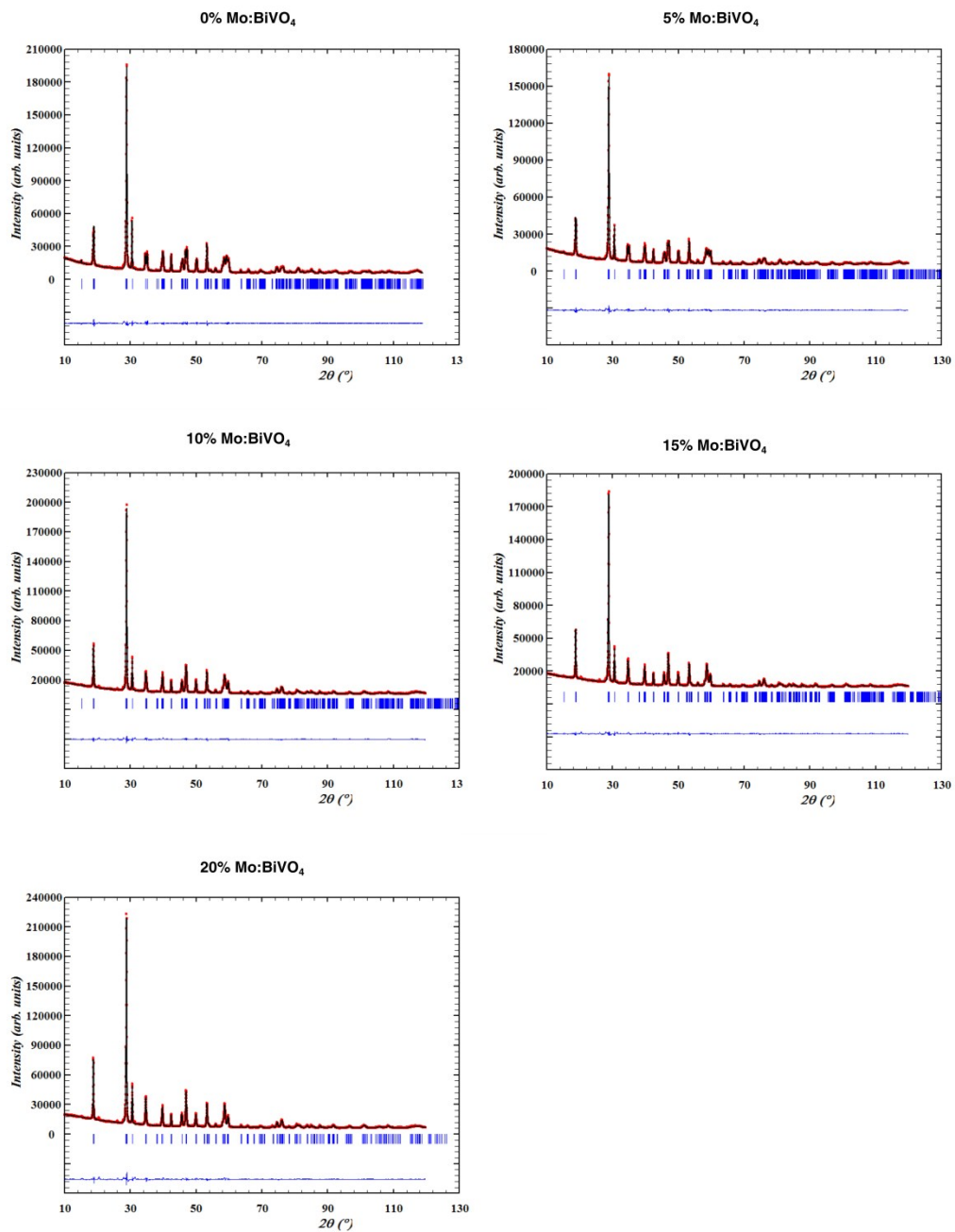


Figure S 5. X-ray powder diffraction patterns of 0%, 5 %, 10 %, 15 % and 20 % Mo:BiVO₄ (from top left to bottom right) with the results of the Rietveld refinements.

Table S 2. Structural parameters for 0%, 5 %, 10 %, 15% and 20 % Mo-BiVO₄ powders.

0% Mo:BiVO ₄	Site	x	y	z	s.o.f.
Bi	4e	0	¼	0.6339(2)	0.998(3)
V	4e	0	¼	0.1279(4)	1.004(3)
O1	8f	0.143(2)	0.4954(14)	0.2103(7)	1
O2	8f	0.2763(14)	0.370(2)	0.4462(7)	1
5 % Mo:BiVO ₄	Site	x	y	z	s.o.f.
Bi	4e	0	¼	0.6291(11)	0.996(2)
V	4e	0	¼	0.1309(4)	0.930(4)*
Mo	4e	0	¼	0.1309(4)	0.070(4)*
O1	8f	0.1458(16)	0.4957(13)	0.2085(7)	1
O2	8f	0.2663(13)	0.3687(17)	0.4493(7)	1
10 % Mo:BiVO ₄	Site	x	y	z	s.o.f.
Bi	4e	0	¼	0.6298(2)	0.964(3)
V	4e	0	¼	0.1314(5)	0.880(4)*
Mo	4e	0	¼	0.1314(5)	0.120(4)*
O1	8f	0.131(2)	0.479(2)	0.2076(9)	1
O2	8f	0.2541(16)	0.378(2)	0.4517(9)	1
15 % Mo:BiVO ₄	Site	x	y	z	s.o.f.
Bi	4e	0	¼	0.63133(15)	0.950(3)
V	4e	0	¼	0.1216(4)	0.836(4)*
Mo	4e	0	¼	0.1216(4)	0.164(4)*
O1	8f	0.133(2)	0.478(2)	0.2069(12)	1
O2	8f	0.250(2)	0.382(3)	0.4498(11)	1
20 % Mo:BiVO ₄	Site	x	y	z	s.o.f.
Bi	4b	0	¼	⁵ / ₈	0.940(6)
V	4a	0	¼	¹ / ₈	0.800(6)*
Mo	4a	0	¼	¹ / ₈	0.200(6)*
O	16f	0.1408(9)	0.0043(7)	0.2044(4)	1

* not refined independently

Table S 3. Reasonable defect models for the substitution of V⁵⁺ by Mo⁶⁺ in BiVO₄ (formal defect equations, Kröger-Vink notation).

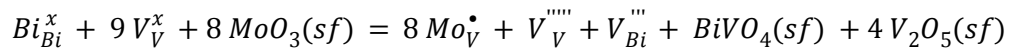
Formation of vanadium vacancies (BiMo_{5x/6}V_{1-x}O₄):



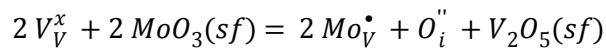
Formation of bismuth vacancies (Bi_{1-x/3}Mo_xV_{1-x}O₄):



Formation of bismuth and vanadium vacancies (Bi_{1-x/9}Mo_{8x/9}V_{1-x}O₄):



Oxygen on interstitial positions (BiMo_xV_{1-x}O_{4+x/2}):



S 5 TEM/SAED of 0%, 10%, 15% and 20% Mo:BiVO₄ samples.

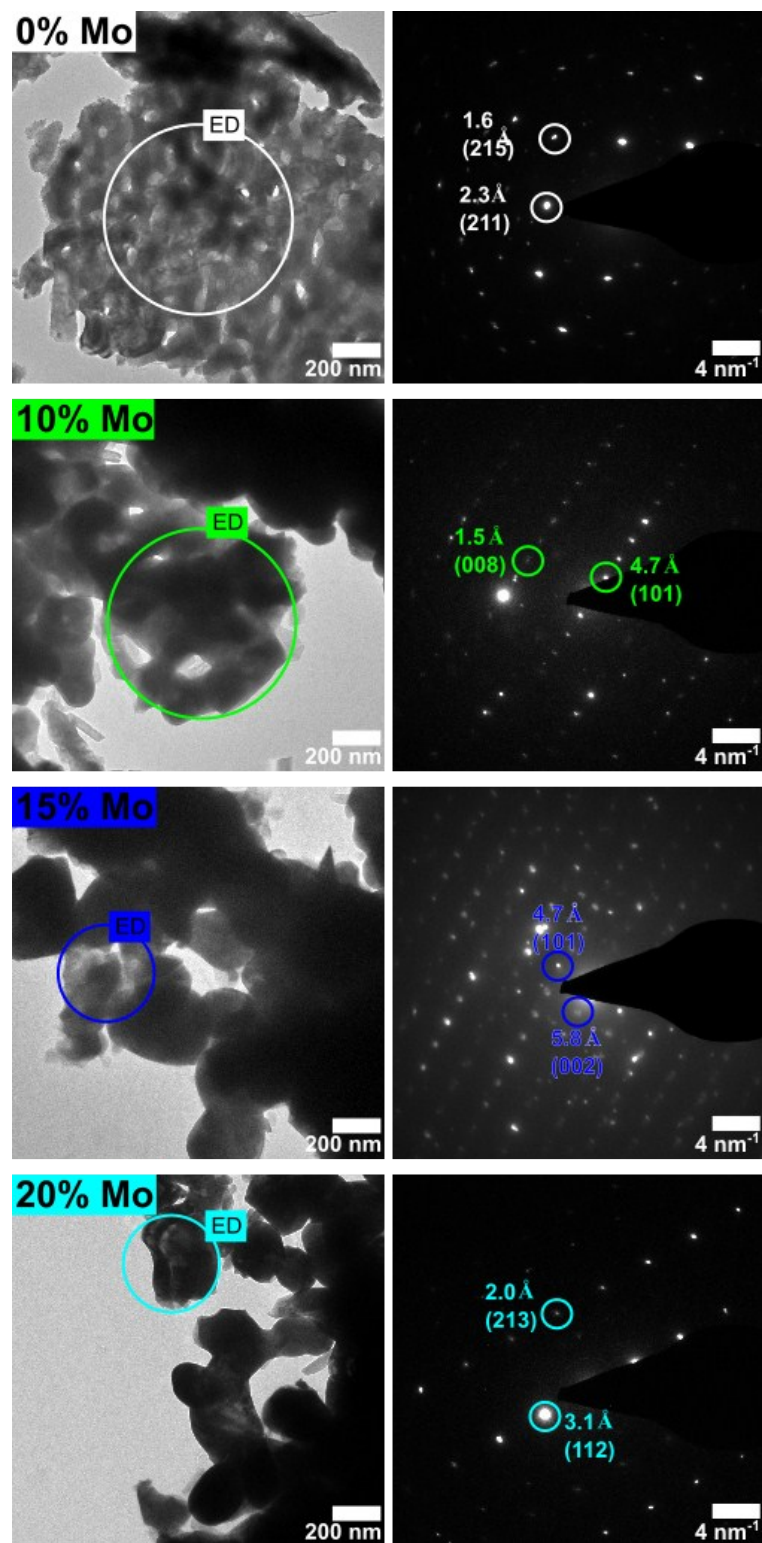


Figure S 6. TEM/SAED of 0%, 10%, 15% and 20% Mo:BiVO₄ samples scraped-off the FTO substrate and transferred to a carbon coated Cu grid. All samples could not be perfectly aligned to zone axis due to fast beam damage of the sample.

S 6 EC-Setup

For electrochemical measurements a standard electrochemical cell was used. The working electrode was connected by copper tape and equipped with an O-ring. The cell was mounted on top of the working electrode allowing an area of 0.5 cm² to get in contact with the electrolyte. A reversible hydrogen electrode (RHE) was used as reference and a platinum wire as counter electrode, respectively. Mounting the light fiber of the light source on top of the EC cell is referred to as front-illumination, i.e. illumination through the electrolyte/BiVO₄/FTO/glass junction. Mounting the light source on the bottom of the cell is referred to as back-illumination, i.e. illumination through the glass/FTO/BiVO₄/electrolyte junction. Light intensity was adjusted to 100 mW/cm² using a light meter equipped with a Si diode.

For Mott-Schottky analysis, a modified Randles circuit consisting of a resistance for voltage drop in the electrolyte R_s , a resistance for charge transfer R_{CT} in series with a Warburg impedance Z_W , which is connected in parallel with a constant phase element Z_{CPE} representative for surface inhomogeneities and the like. Taking into account the total measured impedance of the modified Randles circuit and assuming Z_{CPE} to act as an ideal capacitance, the interfacial capacitance can be represented directly by $1/\sigma$ of Z_{CPE} (see Equation 1).¹

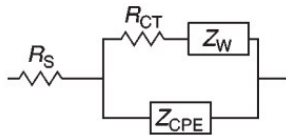


Figure S 7. Modified Randles circuit used for Mott-Schottky analysis.

Equation 1. Impedance of a CPE in an ac circuit with σ as the CPE prefactor, ω as the angular frequency, and m as the CPE exponent.

$$Z_{CPE} = \sigma \omega^{-m} \left[\cos\left(\frac{m\pi}{2}\right) - j \sin\left(\frac{m\pi}{2}\right) \right]$$

S7 j-V-curves of X% Mo:BiVO₄ thin films in frontside and backside illumination

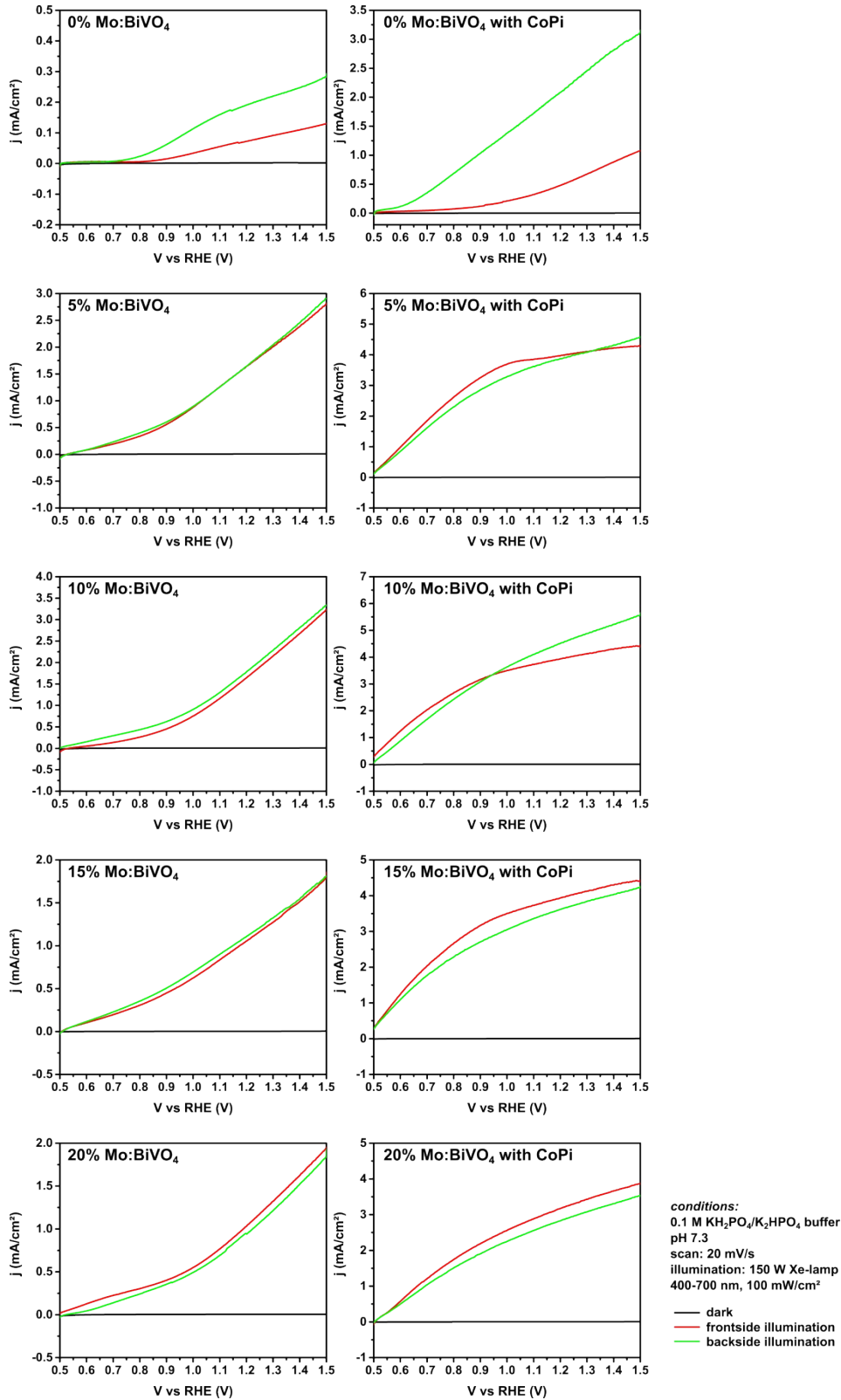


Figure S8. j-V-curves of X% Mo:BiVO₄ thin films with and without CoPi in frontside and backside illumination.

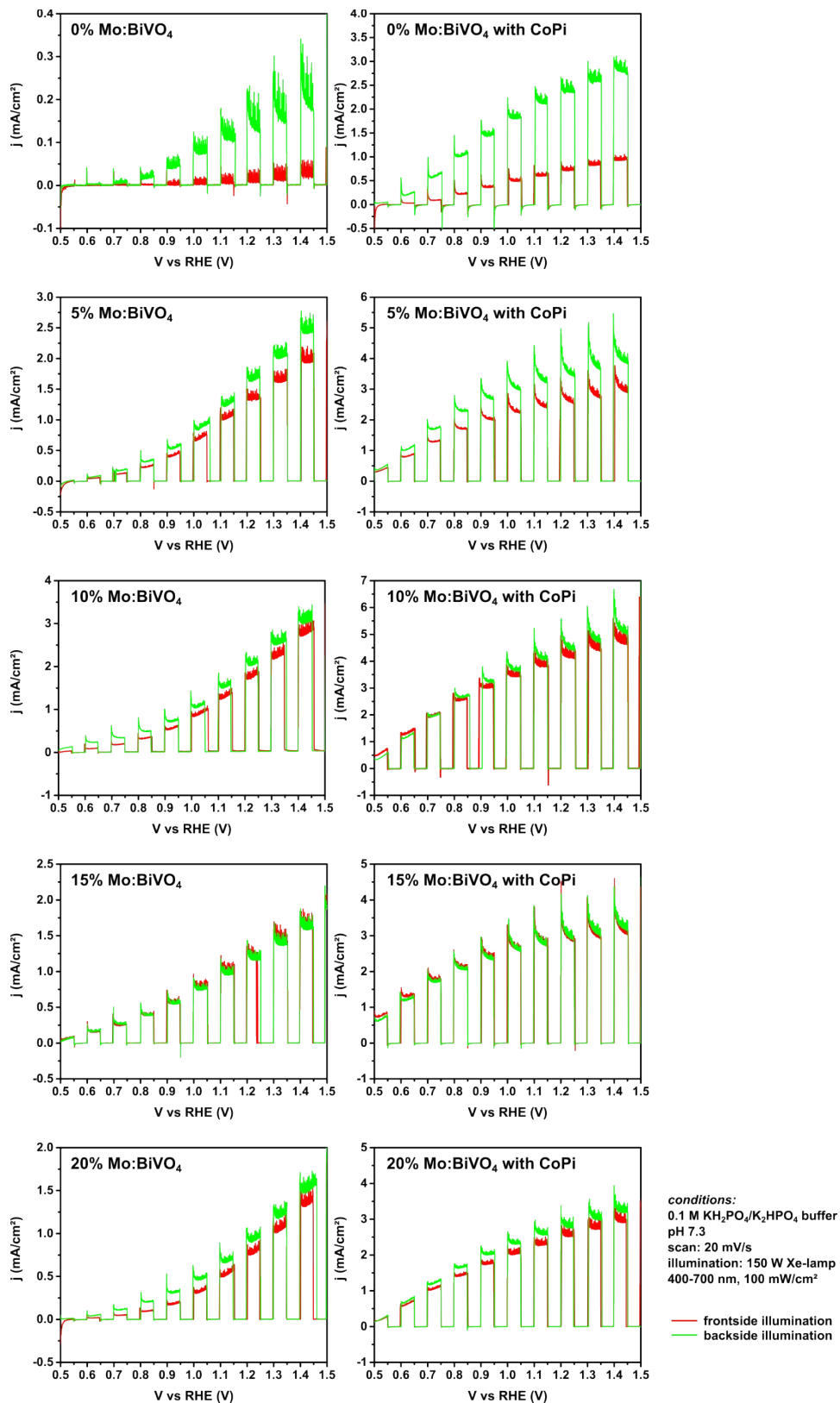


Figure S 9. j-V-curves of X% Mo:BiVO₄ thin films with and without CoPi illuminating with chopped light in frontside and backside mode.

Table S 5. Summary of photocurrents at 1.23 V vs RHE and necessary potential to yield photocurrents of 1.0 mA/cm².

	j at 1.23 V vs RHE (mA/cm ²)				V vs RHE at j = 1.0 mA/cm ² (V)			
	without co-catalyst		with CoPi		without co-catalyst		with CoPi	
	frontside	backside	frontside	backside	Frontside	backside	frontside	backside
0% Mo:BiVO ₄	0.08	0.23	0.51	2.20	-	-	1.47	0.90
5% Mo:BiVO ₄	1.75	1.75	4.01	3.93	1.03	1.03	0.60	0.61
10% Mo:BiVO ₄	1.89	1.93	3.51	4.63	1.06	1.01	0.63	0.62
15% Mo:BiVO ₄	1.13	1.17	4.00	3.69	1.19	1.17	0.57	0.59
20% Mo:BiVO ₄	1.12	1.02	3.25	2.91	1.19	1.23	0.66	0.69

S 8 Faradaic efficiency determination

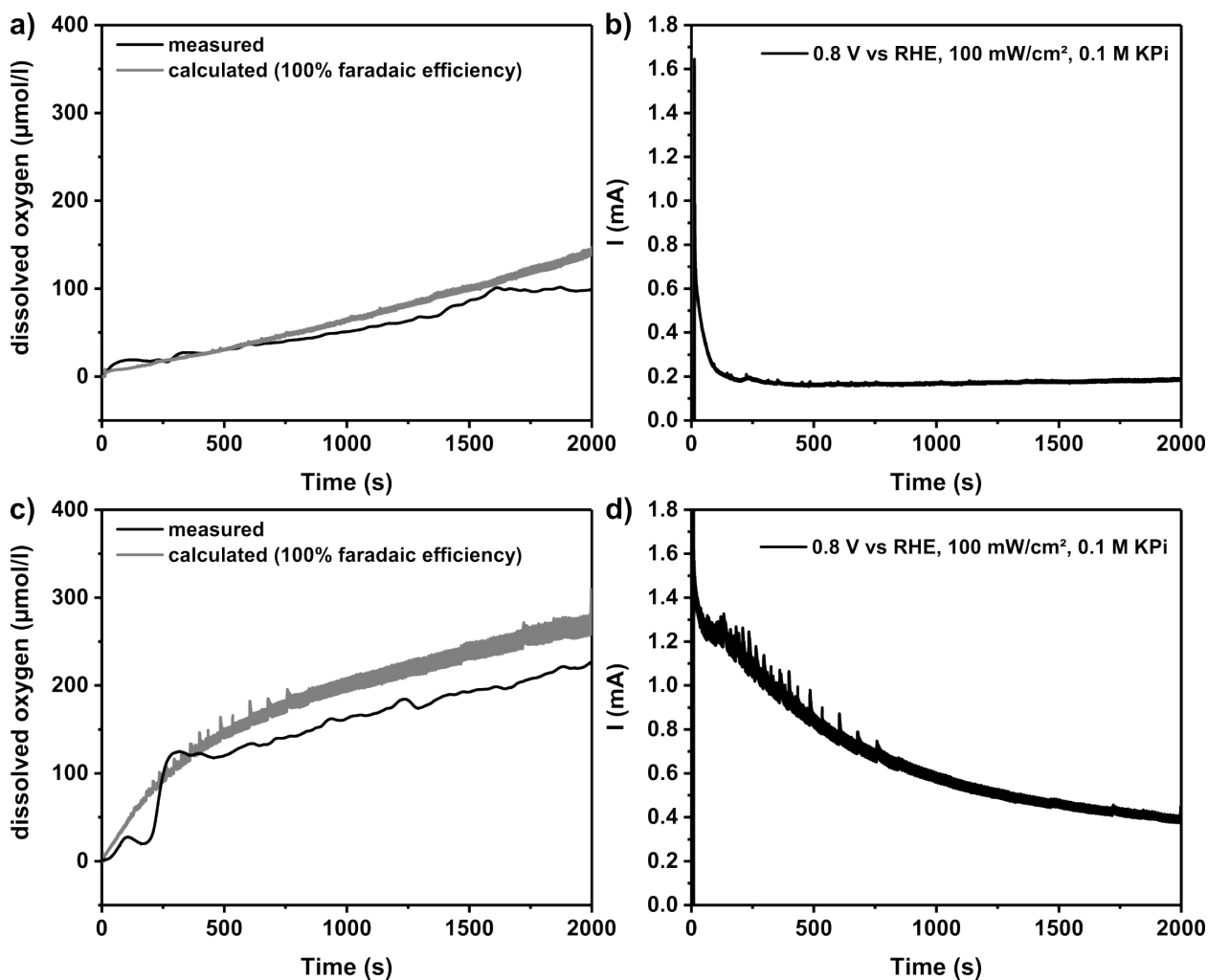


Figure S 10. Determination of dissolved oxygen by usage of a Clark electrode for a 10%Mo:BiVO₄ electrode during electrolysis at 0.8 V vs RHE and under illumination of white light (400-700 nm) at 100 mW/cm² over a time period of 50 min. a) dissolved oxygen vs. time without CoPi deposited at the surface, b) corresponding current vs. time without CoPi deposited, c) dissolved oxygen vs. time with CoPi deposited at the surface, d) corresponding current vs. time with CoPi deposited.

The theoretical O₂ amount was calculated according to the number of the transferred electrons (assuming 100% faradaic efficiency). The faradaic efficiency was calculated by comparing the experimentally observed O₂ amount with that obtained by the theoretical results.

Faradaic efficiencies for the 10% Mo:BiVO₄ photoanodes of 93% and 88% before and after CoPi deposition, respectively, are in good agreement with literature reporting faradaic efficiencies regarding water oxidation for comparable BiVO₄-based photoanodes ranging from 79% to 96%.

Table S 4. Literature reports on faradaic efficiency of different BiVO₄-based photoanodes.

Author	Photoanode	O ₂ determination	Faradaic efficiency
Rao et al. ²	WO ₃ /BiVO ₄ Core-Shell Nanowire	Gas chromatography	79%
Tang et al. ³	BiVO ₄ /CdTe/Co(OH) ₂	Fluorescent probe	90%
Zhang et al. ⁴	Mo:BiVO ₄ /Au	Gas chromatography	95%
Kim et al. ⁵	N ₂ -treated BiVO ₄	Gas chromatography	96%
Present work	Mo:BiVO ₄	Clark electrode	93%
Present work	Mo:BiVO ₄ /CoPi	Clark electrode	88%

S 9 Photocurrent transients for X% Mo:BiVO₄ thin films in frontside and backside illumination

Table S 6. Summary of results of photocurrent transient analysis.

0% Mo:BiVO ₄	without CoPi	j _{ini} = 0.055 mA/cm ²	η _{transfer} = 0.033	k _{trans} = 0.040
		j _{ss} = 0.002 mA/cm ²		k _{rec} = 1.189
	with CoPi	j _{ini} = 0.097 mA/cm ²	η _{transfer} = 0.191	k _{trans} = 0.105
		j _{ss} = 0.018 mA/cm ²		k _{rec} = 0.446
5% Mo:BiVO ₄	without CoPi	j _{ini} = 0.225 mA/cm ²	η _{transfer} = 0.445	k _{trans} = 0.274
		j _{ss} = 0.100 mA/cm ²		k _{rec} = 0.341
	with CoPi	j _{ini} = 0.341 mA/cm ²	η _{transfer} = 0.844	k _{trans} = 0.356
		j _{ss} = 0.288 mA/cm ²		k _{rec} = 0.066
10% Mo:BiVO ₄	without CoPi	j _{ini} = 0.267 mA/cm ²	η _{transfer} = 0.477	k _{trans} = 0.170
		j _{ss} = 0.127 mA/cm ²		k _{rec} = 0.186
	with CoPi	j _{ini} = 0.563 mA/cm ²	η _{transfer} = 0.877	k _{trans} = 0.302
		j _{ss} = 0.494 mA/cm ²		k _{rec} = 0.042
15% Mo:BiVO ₄	without CoPi	j _{ini} = 0.168 mA/cm ²	η _{transfer} = 0.438	k _{trans} = 0.275
		j _{ss} = 0.074 mA/cm ²		k _{rec} = 0.345
	with CoPi	j _{ini} = 0.393 mA/cm ²	η _{transfer} = 0.629	k _{trans} = 0.481
		j _{ss} = 0.247 mA/cm ²		k _{rec} = 0.284
20% Mo:BiVO ₄	without CoPi	j _{ini} = 0.199 mA/cm ²	η _{transfer} = 0.528	k _{trans} = 0.233
		j _{ss} = 0.105 mA/cm ²		k _{rec} = 0.208
	with CoPi	j _{ini} = 0.278 mA/cm ²	η _{transfer} = 0.687	k _{trans} = 0.386
		j _{ss} = 0.191 mA/cm ²		k _{rec} = 0.176

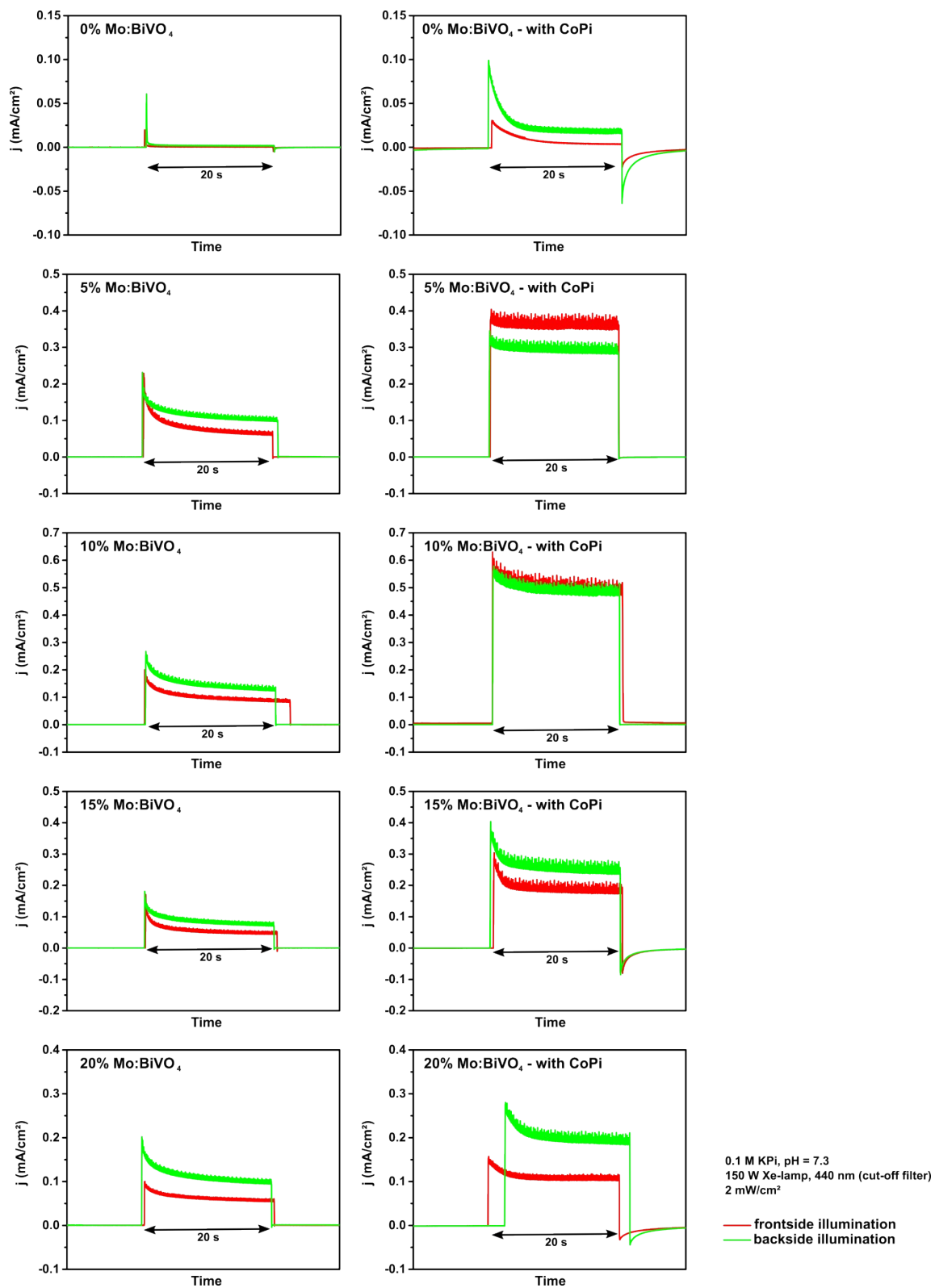


Figure S 11. Photocurrent transients for X% Mo:BiVO₄ thin films acquired at an applied potential of 1.23 V vs RHE in frontside and backside illumination.

References

- 1 K. Gelderman, L. Lee and S. W. Donne, *J. Chem. Educ.*, 2007, **84**, 685.
- 2 P. M. Rao, L. Cai, C. Liu, I. S. Cho, C. H. Lee, J. M. Weisse, P. Yang and X. Zheng, *Nano letters*, 2014, **14**, 1099–1105.
- 3 Y. Tang, R. Wang, Y. Yang, D. Yan and X. Xiang, *ACS applied materials & interfaces*, 2016, **8**, 19446–19455.
- 4 L. Zhang, C.-Y. Lin, V. K. Valev, E. Reisner, U. Steiner and J. J. Baumberg, *Small (Weinheim an der Bergstrasse, Germany)*, 2014, **10**, 3970–3978.
- 5 T. W. Kim, Y. Ping, G. A. Galli and K.-S. Choi, *Nature communications*, 2015, **6**, 8769.